J Appl Electrochem (2008) 38:731–742
DOI 10.1007/s10800-008-9536-0

REVIEW IN APPLIED ELECTROCHEMISTRY NUMBER 65

Advances in electrochemical Fe(VI) synthesis and analysis

Xingwen Yu · Stuart Licht

Received: 30 May 2007 / Revised: 17 February 2008 / Accepted: 25 February 2008 / Published online: 8 March 2008

Abstract Hexavalent iron species (Fe(VI)) have been known for over a century, and have long-time been investigated as the oxidant for water purification, as the catalysts in organic synthesis and more recently as cathodic charge storage materials. Conventional Fe(VI) syntheses include solution phase oxidation (by hyphchlorite) of Fe(III), and the synthesis of less soluble super-irons by dissolution of FeO_4^{2-}, and precipitation with alternate cations. This paper reviews a new electrochemical Fe(VI) synthesis route including both in situ and ex situ syntheses of Fe(VI) salts. The optimized electrolysis conditions for electrochemical Fe(VI) synthesis are summarized. Direct electrochemical synthesis of Fe(VI) compounds has several advantages of shorter synthesis time, simplicity, reduced costs (no chemical oxidant is required) and providing a possible pathway towards more electro-active and thermal stable Fe(VI) compounds. Fe(VI) analytical methodologies summarized in this paper are a range of electrochemical techniques. Fe(VI) compounds have been explored as energy storage cathode materials in both aqueous and non-aqueous phase in "super-iron" battery configurations. In this paper, electrochemical synthesis of reversible Fe(VI/III) thin film towards a rechargeable super-iron cathode is also summarized.

Keywords Fe(VI) · Electrochemical synthesis · Electrochemical analysis · Reversible Fe(VI/III) thin film

X. Yu (✉)
Department of Chemical and Biological Engineering,
The University of British Columbia, 2360 East Mall, Vancouver,
BC, Canada V6T 1Z3
e-mail: xingwenyu@yahoo.com

S. Licht
Department of Chemistry, University of Massachusetts, Boston,
MA 02125, USA

1 Introduction

Although Hexavalent iron species have been known for over a century, Fe(VI) chemistry is not as established as that for ferrous, Fe(II), ferric, Fe(III) or zero valent (metallic) iron chemistry. However, it has been a long-time investigation of using Fe(VI) as the oxidant for water purification [1–8], as the catalysts in organic synthesis [9], and more recently as cathodic charge storage materials [10–50].

In conventional chemical syntheses, high purity, stable K_2FeO_4 is prepared, from alkaline hypochlorite oxidation of Fe(III), and less soluble Fe(VI) salts are prepared by precipitation, upon addition of various salts to solutions containing dissolved FeO_4^{2-} [16, 17]. Electrochemical methodologies for Fe(VI) synthesis have recently been developed [23, 28, 30, 31, 34, 51–55]. At potentials greater than 0.6 V versus SHE (standard hydrogen electrode) in alkaline media, an iron metal anode can be directly oxidized to FeO_4^{2-}. Early attempts to electrochemically synthesize Fe(VI) compounds have focused on the anodic dissolution of an iron metal anode into a solution, and the solution phase FeO_4^{2-} was then used to prepare other Fe(VI) salts (This approach was named as ex situ synthesis). When the electrolyte contains an Fe(VI) precipitating cation, the generated FeO_4^{2-} can be rapidly isolated as a solid, and stabilized ferrate salt (This approach was named as in situ synthesis). So far, solid K_2FeO_4 and $BaFeO_4$ have been successfully synthesized through this in situ electrochemical synthesis rout [23, 28, 31, 54, 55]. The one-step direct electrochemical synthesis (in situ electrochemical synthesis) of solid Fe(VI) salts has significant advantages in shorter synthesis time, simplicity, and reduced costs (no chemical oxidant is required). This paper provide a review of recent advances in electrochemical Fe(VI) synthesis (including both ex situ and in situ synthesis).

Fe(VI) salts have been introduced as novel charge storage super-iron cathodes [10–50]. These salts exhibit up to three electrons of charge storage occurring at a single, electropositive cathodic potential. Whereas primary charge transfer has been extensively demonstrated, reversible charge transfer of Fe(VI) salts has been problematic. Thin film Fe(III/VI) cathode can facilitate electronic communication with a conductive substrate to sustain cycled charge storage. This paper also summaries the recent progresses of electrochemical preparation of reversible Fe(VI/III) thin films.

Electroanalytical techniques to probe Fe(VI) compounds can be conveniently categorized as either solution phase (dissolved Fe(VI)) or solid cathode techniques. The solution electrochemical techniques for Fe(VI) analyses, including potentiometric analysis, galvanostatic analysis and cyclic-voltammetry, are also summarized in this paper.

2 Fundamentals of electrochemical Fe(VI) synthesis

Conventionally, Fe(VI) has always been prepared from alkaline hypochlorite oxidation of Fe(III) salts [10, 16, 17]. However, at sufficiently anodic potentials, an iron (metal) anode can be directly oxidized to the Fe(VI) species (FeO_4^{2-}) in alkaline media, in accord with the oxidation reaction [31]:

$$Fe + 8OH^- \rightarrow FeO_4^{2-} + 4H_2O + 6e^- \quad (1)$$

This process occurs at potentials >0.6 V versus the standard hydrogen electrode, SHE, consistent with the alkaline rest potentials related to the formation of Fe(II), Fe(III) and Fe(VI) from Fe(0) [3, 31]:

$$Fe + 2OH^- \rightarrow Fe(OH)_2 + 2e^-; \quad E^\circ = -0.8 \text{ V versus SHE} \quad (2)$$

$$Fe(OH)_2 + OH^- \rightarrow FeOOH + H_2O + e^-; \quad E^\circ = -0.7 \text{ V versus SHE} \quad (3)$$

$$FeOOH + 5OH^- \rightarrow FeO_4^{2-} + 3H_2O + 3e^-; \quad E^\circ = +0.6 \text{ V versus SHE} \quad (4)$$

With Fe(VI) formation, isolation of generated Fe(VI) away from the cathode will minimize the Fe(VI) loss due to the cathodic back-reduction of the synthesized Fe(VI), Eq. 5, and instead favoring the cathodic evolution of hydrogen, Eq. 6 [23, 31]:

$$FeO_4^{2-} + 3H_2O + 3e^- \rightarrow FeOOH + 5OH^- \quad (5)$$

$$6H_2O + 6e^- \rightarrow 6OH^- + 3H_2 \quad (6)$$

With 6 Faraday of charge transfer through the anode and cathode per equivalent of Fe, Eqs. 1 and 6 combined yield the net Fe(VI) solution phase alkaline synthesis reaction [31]:

$$Fe + 2OH^- + 2H_2O \rightarrow FeO_4^{2-} + 3H_2 \quad (7)$$

Early attempts to electrochemically synthesize Fe(VI) compounds have focused on the anodic dissolution of an iron metal anode into a solution. Less soluble Fe(VI) salts were then synthesized in an 'ex situ' way through chemical precipitation reaction [31, 34, 51]. This ex situ electrochemical synthesis rout is generalized on the left side of Fig. 1 ($BaFeO_4$ synthesis is shown here as an example).

The alternative path (in situ rout) to the electrochemical synthesis of solid Fe(VI) salts is presented as the right side of Fig. 1. In the in situ synthesis, Fe(VI) is electrochemically generated in the alkaline solution containing the cations for Fe(VI) precipitation, and less soluble Fe(VI) compounds precipitates directly in the electrochemical cell. In principle, this direct electrochemical synthesis has several advantages. Fewer preparatory steps should reduce requisite synthesis time and can increase the yield of the Fe(VI) salt. Fe(VI) solutions are susceptible to degradation to Fe(III) due to trace Ni(II) and Co(II) catalysis [10]. This may be avoided during Fe(VI) salt preparation, by strict control over solution impurities, but it will be less complex to avoid this issue by minimizing solution contact time. These and other advantages include (1) Fe(VI) synthesis is simplified to a one step process; (2) Fe(VI) instability is avoided through the direct formation of the solid product; (3) On a volumetric basis, the product is formed at several orders of magnitude higher concentration than for solution phase generation; (4) The system avoids the consumption of chemical oxidants used in chemical Fe(VI) synthesis; (5) The electrolytic generation of solid super-iron salts may provide pathways for more electro-active Fe(VI) compounds.

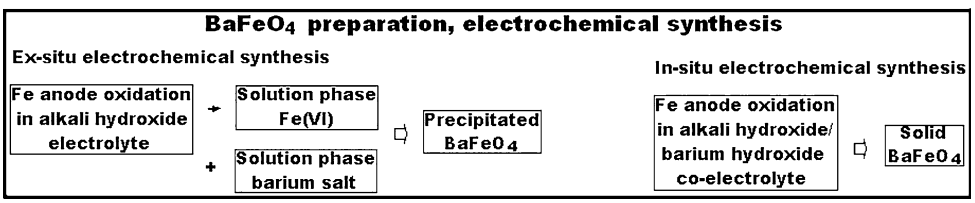

Fig. 1 Scheme of ex situ (left) and in situ (right) electrochemical syntheses for $BaFeO_4$

3 Electrochemical solution phase Fe(VI) generation and optimization

Electrochemically synthesis of solution phase FeO_4^{2-} has generally been conducted with a two compartment electrolysis cell separated with an anion impermeable membrane. High surface area iron (wire, sheet, particles) has normally been used as the anode. Electrolyte was generally high-concentration alkaline solution (NaOH or KOH). Fe(VI) yield is strongly related to various synthesis parameters including: (1) anode materials; (2) separator; (3) alkaline electrolyte; (4) anodic current density; (5) temperature and (6) electrolysis time etc. Optimization of Electrochemical solution phase Fe(VI) generation has recently been systematically studied [23, 28, 31, 30, 52, 53]. As previously reported, NaOH electrolytes support higher solution Fe(VI) production rates and efficiencies than KOH electrolyte [56–58] at low temperature. Therefore, in most solution phase Fe(VI) generation studies at low temperature, NaOH was generally used as the alkaline electrolyte [23, 28, 31, 30, 52, 53].

De Koninek et al. studied the effect of anode materials on the Fe(VI) solution phase generation [30, 52]. They used a pressed iron powder electrode and an iron foil electrode to compare the effect of porosity on the yield of Fe(VI) generation. As summarized in Table 1, the beneficial effect of a porosity increase of an iron electrode on the rate of electrochemical Fe(VI) formation was evident [52]. De Koninek et al. also proved that the pressure applied to the iron powder during the formation of the pellet electrode did not have a strong influence on ferrate generation. On the other hand, the purity, particle size and packing density of the powders are important factors in determining the current yield for ferrate generation [30].

Figure 2 summarizes several electrolyte and membrane effects on solution phase generation of Fe(VI) in alkaline electrolytes. The isolation of the cathode in a separate compartment with a membrane substantially increases the rates and concentration of Fe(VI) production. Isolation of Fe(VI) away from the cathode minimizes losses due to the cathodic reduction of the synthesized Fe(VI), and instead favoring the cathodic evolution of hydrogen [58]. Also NaOH electrolytes exhibits better efficiency effects for solution Fe(VI) generation than that of KOH electrolyte at the studied temperature [31].

Table 1 Comparison of the CV data of the iron pellet electrode and the iron foil electrode [52]

E (V, versus Hg/HgO)	J_{pellet} (mA cm^{-2})	J_{foil} (mA cm^{-2})	J_{pellet}/J_{foil}
−1.36	106	4.7	23
−0.42	66	1.6	41
0.1	61	1.0	61
0.6	40	1.1	36
0.97	105	3.8	28

The effect of the solution-phase cation on the kinetics of Fe oxidation to Fe(VI) will be governed by competing factors which include the solubilities of Fe(VI) in different electrolytes [10, 11, 15, 19], and also those of the Fe(II) and Fe(III) intermediate products which tend to be less soluble and can passivate the anode surface, and alter the surface morphology. The Li, Na and K comparative cation effect has been probed at lower concentrations than 12 or 14 M [31]. Limited by the ~5 M solubility of LiOH, equimolar Na, K and Li hydroxide electrolytes were utilized for Fe(VI) electrochemical synthesis, under the same electrolysis conditions [31]. As with the more concentrated electrolytes, the average rate of Fe(VI) formation in 5 M NaOH (an hourly rate of 15 mM h^{-1}) is significantly faster and more efficient than in the 5 M KOH (9.7 mM h^{-1}), or in 5 M LiOH (0.3 mM h^{-1}), and the Na cation electrolyte is clearly preferred for rapid Fe(VI) synthesis [31].

NaOH concentration effect on the Fe(VI) electrochemical generation has been well studied, and 14–16 M NaOH was proved to have the best effect for the Fe(VI) yield [23, 28, 31, 30, 52, 53]. The enhanced rate of formation in the high-concentration compared to the low-concentration NaOH electrolyte is attributed to the pH-dependent redox couple Eq. 1, governed by a Le Chatelie increase in the hydroxide availability. Furthermore, there is a decrease in the free water activity of high-concentration compared to low-concentration alkaline medium [59], which can inhibit losses of Fe(VI) due to parasitic decomposition in accord with Eq. 8, and diminish the kinetics of the competing anodic evolution of oxygen Eq. 9:

$$4FeO_4^{2-} + 2H_2O \rightarrow 4FeO_2^{-} + 3O_2 + 4OH^- \quad (8)$$

$$2H_2O \rightarrow O_2 + 4H^+ + 4e^- \quad (9)$$

Figure 3a is an example of a closer inspection of the concentration effect in NaOH electrolytes, which exhibits high efficiency Fe(VI) formation rate for a 14 M solution at a synthesis current density of 2.0 mA cm^{-2} [31]. Electrolyte specific conductivity has a maximum at intermediate high concentrations and falls off in saturated hydroxide electrolytes [60]. Therefore, the observed synthesis rate decreases in the 18 M NaOH electrolyte, and parallels the falloff in conductivity as the electrolyte nears saturation, which will constrain reactant (hydroxide) mass transport to the electrode. Furthermore, with the electrolysis going on, the cell is subject to IR heat, and the internal cell temperature will rise. The internal cell temperature exhibits an inverse variation with the electrolyte specific conductivity, and affects the rate and efficiency of synthesis. But the increased

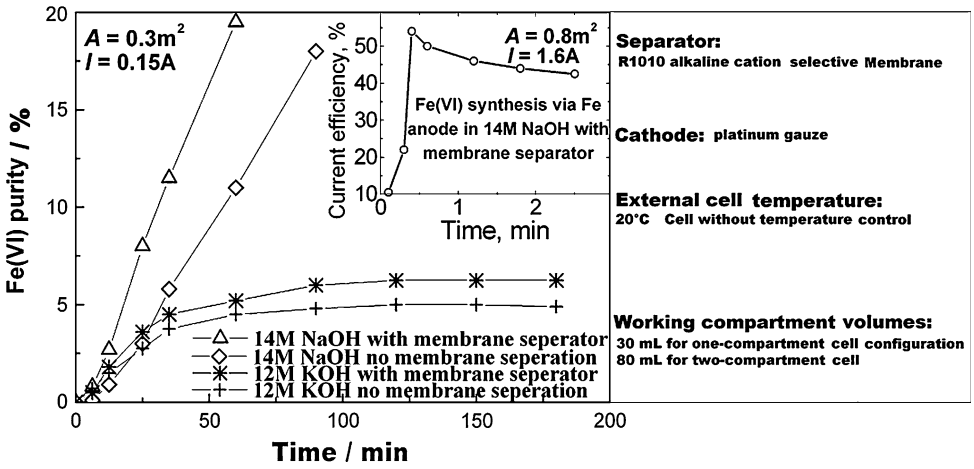

Fig. 2 Electrochemical Fe(VI) formation at constant current density from an Fe anode; increase in time of the FeO_4^{2-} concentration. The effect of electrolyte and of a cation selective membrane separation of the Fe and counter electrodes, to exclude synthesized Fe(VI) from the counter electrode. Inset: the variation of current efficiency with the electrolysis time for Fe(VI) formation [31]

internal cell temperature also increases the rate of parasitic Fe(VI) losses described in Eq. 8 [31]. He et al. investigated the influences of NaOH concentration and anodic current density on ferrate(VI) yield [53]. In this study, the optimal NaOH concentration was found to be 14–16 M (as summarized in Fig. 3b). He et al. also explained that the decrease of the Fe(VI) yield with increasing current density was caused by the increase in the oxygen evolution rate becoming larger than that in ferrate(VI) electrogeneration rate with the increase of current density [53]. In addition, a peak value of Fe(VI) yield occurs at the current density of 4.32 mA cm^{-2} in 15.01 and 16.32 M NaOH solutions, which might result from the increased solubility of lower valence iron species in the anolyte with increasing alkalinity [53, 61]. From the comprehensive effect of different factors, Licht's group considered the 2 mA cm^{-2} as the optimal anode current density [23, 28, 31].

Licht's group studied the substantial effect of temperature on Fe(VI) electrochemical synthesis [31]. Increasing the cell temperature generally results in faster rates of Fe(VI) synthesis. However, this trend is diminished or reverses for temperatures higher than 35 °C, which is particularly evident at the longer synthesis time (as summarized in Fig. 4a). These observations are consistent with the competition between enhanced synthesis and decomposition rates expected for FeO_4^{2-} at elevated temperatures, resulting in the observed maximum at ~35 °C [31]. In order to obtain a high concentration of ferrate(VI) solution during electrolysis, it is indispensable to develop a rapid synthesis method due to the instability of ferrate(VI). He et al. studied the kinetics of competitive formation and decomposition of Fe(VI) during the electrolysis [53]. The dependences of ferrate(VI) concentration ($[FeO_4^{2-}]$), apparent ferrate(VI) yield (η_{app}), NaOH concentration ($[OH^-]$) and lower valence iron content (ΣFe-$[FeO_4^{2-}]$) on electrolysis duration are summarized in Fig. 4b. The highest η_{app} occurs in the first hour and then decreases with electrolysis time [53].

4 Ex situ electrochemical synthesis of $BaFeO_4$

Ex situ Fe(VI) synthesis starts with electrochemically generated, solution phase FeO_4^{2-}. When the FeO_4^{2-}

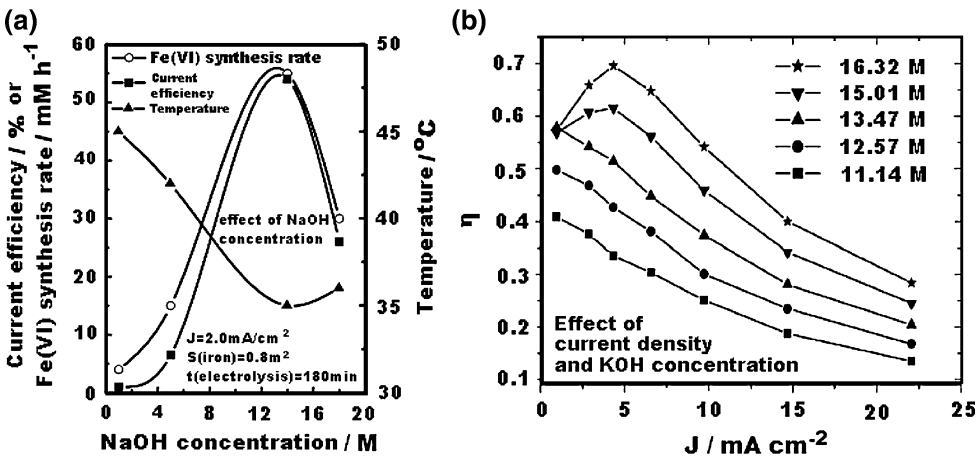

Fig. 3 Electrochemical synthesis of solution phase FeO_4^{2-}. (**a**) The effect of NaOH concentration on average Fe(VI) synthesis rate, maximum anodic current efficiency, and the maximum monitored internal cell temperature. (**b**) Dependence of ferrate(VI) yield (η) on NaOH concentration and anodic current density [31, 53]

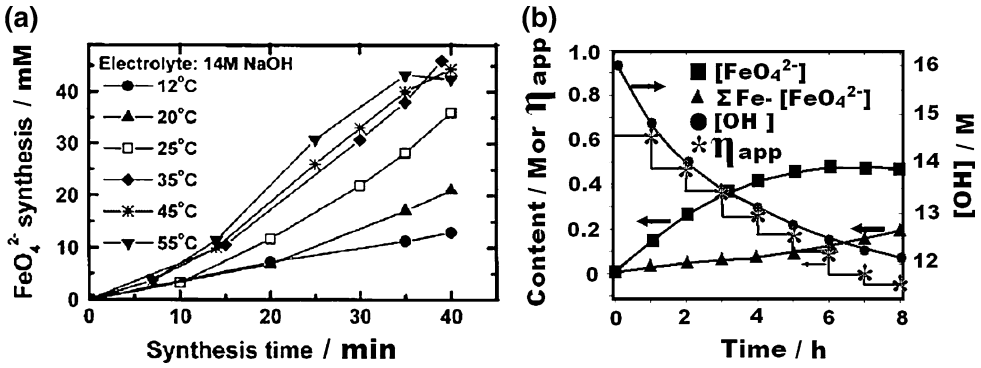

Fig. 4 (**a**) Controlled temperature, electrochemical synthesis of FeO_4^{2-}: the time dependent variation of Fe(VI) concentration in solution. (**b**) Content of some components or η_{app} as a function of time during a continuous electrolysis of iron in 16 M NaOH. The η_{app} is the average apparent yield of Fe(VI) in 1 h [31, 53]

concentration in solution increases to a desired value, the solution is removed and mixed with another solution containing $Ba(OH)_2$. $BaFeO_4$ rapidly precipitates due to its low solubility compared to Na_2FeO_4:

$$Na_2FeO_4 + Ba(OH)_2 \rightarrow BaFeO_4 + 2NaOH \quad (10)$$

Licht's group studied the ex situ $BaFeO_4$ synthesis [31] as summarized in Table 2. In the ex situ synthesis cases, the $BaFeO_4$ yield and purity generally are high in 10 and 14 M NaOH electrolyte. The reason that no significant beneficial for 14 M NaOH compared to 10 M NaOH might attribute to the impurities in the product including the remains of barium oxide, hydroxide or carbonate that are not washed away.

In an attempt to further increase the $BaFeO_4$ product purity, Licht et al. varied the molar ratio between the $Ba(OH)_2$ and iron reactants. Yields of $BaFeO_4$ were best when substoichiometric amounts of barium hydroxide were used. Decreasing of the molar ratio between $Ba(OH)_2$ and FeO_4^{2-} also enhances the product's purity (as described in Table 2). The optimal temperature for this ex situ synthesis is marginally better at 25 °C, rather than the expected 35 °C, in terms of purity, yield, and synthesis efficiency [31].

5 In situ electrochemical synthesis of $BaFeO_4$

A simpler, effective alternative to the ex situ electrochemical generation of $BaFeO_4$ is the in situ synthesis. In the in situ synthesis the $Ba(OH)_2$ reactant is included in the initial electrolysis cell, in which FeO_4^{2-} ions are continuously generated at the anode as an electro-oxidative addition. The spontaneous anodic reaction is therefore:

$$Fe + 6OH^- + Ba(OH)_2 \rightarrow BaFeO_4 + 4H_2O + 6e^- \quad (11)$$

And in accord with Eq. 6, the net cell reaction becomes:

$$Fe + Ba(OH)_2 + 2H_2O \rightarrow BaFeO_4 + 3H_2 \quad (12)$$

In a pure (NaOH-free) aqueous $Ba(OH)_2$ electrolyte, little Fe(VI) can be generated electrochemically. This is evidently limited by the comparatively low concentration of OH^- sustainable in such solutions. In the pure aqueous $Ba(OH)_2$ electrolyte, the maximum concentration of solution-phase hydroxide ($[OH^-] < 0.5$ M) is limited by the saturation of $Ba(OH)_2$, which is insufficient to sustain high rates of Fe(VI) formation. The solubility of $Ba(OH)_2$ is 0.2 M at room temperature and falls significantly with added NaOH. However, the synthesis can progress rapidly

Table 2 Ex situ electrochemical syntheses of $BaFeO_4$ under a variety of physical and chemical conditions [31]

[NaOH] (M)	Electrolysis time (min)	Internal temperature (°C)	n_{Ba}/n_{Fe} in reactants	Theoretical $BaFeO_4$ produced (mmol)	$BaFeO_4$ purity (%)	Yield (%)	Synthesis efficiency (%)
8	110	25	2.0:1.0	3.04	82.7	77.1	63.8
10	60	25	2.0:1.0	2.82	84.1	77.4	65.1
10	50	25	1.0:1.0	2.43	84.5	86.6	73.2
10	105	25	1.0:1.5	3.40	90.5	93.0	84.2
10	85	25	1.0:3.0	1.39	89.4	97.7	87.3
14	110	12	2.0:1.0	2.50	70.4	92.1	64.8
14	60	20	2.0:1.0	2.32	76.6	92.0	70.4
14	50	25	2.0:1.0	3.50	78.5	98.9	77.6
14	45	35	2.0:1.0	3.60	73.1	96.4	70.5
14	30	45	2.0:1.0	2.50	70.1	87.3	61.2
14	35	55	2.0:1.0	3.00	68.3	67.9	46.4
18	60	25	2.0:1.0	2.64	77.9	97.4	75.9

in an aqueous sodium/barium hydroxide co-electrolyte, forming at rates comparable to the pure NaOH electrolyte [31].

Licht's group systematically studied the in situ $BaFeO_4$ electrochemical synthesis [23, 28, 31]. Table 3 summarizes a series of these in situ electrochemical syntheses performed in 10 or 14 M NaOH electrolytes. Increasing the NaOH concentration from 10 to 14 M in the in situ synthesis leads to improvements of both purity and yield of $BaFeO_4$. It is significant that the $BaFeO_4$ prepared in situ generates a significantly higher purity than the ex situ prepared product (compared Tables 2 and 3). Also evident in Table 3 is the effect of varying the molar ratio between the FeO_4^{2-} and $Ba(OH)_2$ reactants. Increasing the FeO_4^{2-} content leads to a minor improvement of both purity and yield of $BaFeO_4$. Increasing this ratio above 50% induces a decrease in the purity, although accompanied by an increase in the yield. The cause for these observations lies in the relatively longer time required for such synthesis. After a lengthy electrolysis, Fe(III) can accumulate. This directly affects the purity and the total mass of the contaminated product. Also in these studies, optimized in situ electrochemically synthesized $BaFeO_4$ was obtained during 70 min of 1.6 A electrolysis in a co-electrolyte of 14 M NaOH and 45 mM $Ba(OH)_2$ at 45 °C [31].

Figure 5 compares FTIR and XRD spectra of the high purity chemical, compared to in situ electrochemical, synthesis of $BaFeO_4$. Both analyses present nearly identical crystalline diffraction patterns [consistent with the space group $D2h$ (*Pnma*)] [24] and IR absorption spectra (including the well-defined, typical $BaFeO_4$ triplet at 750–800 cm^{-1}). These measurements also verify that high purity $BaFeO_4$ was obtained employing the electrochemical optimized preparation procedure.

Table 4 summaries the chemical and electrochemical synthesis of $BaFeO_4$. One major difference in the methodologies is in the synthesis temperature. Whereas the chemical synthesis of K_2FeO_4 and its conversion to $BaFeO_4$ are performed at low temperatures to avoid decomposition, both in situ and ex situ electrochemical syntheses require higher temperature (25–45 °C) to facilitate the Fe(VI) electrolysis. Under such conditions, the electrochemical syntheses are one to two orders of magnitude faster than the chemical synthesis, providing an advantage. In situ electrochemical synthesis is the simplest methods, requiring only a single reaction step. The in situ $BaFeO_4$ purity obtained is high, often approaching the purity of the chemical synthesis. Although providing a less pure product, the yield of the ex situ synthesis is also high (93–98%) and can significantly surpass that of the in situ electrochemical methodology.

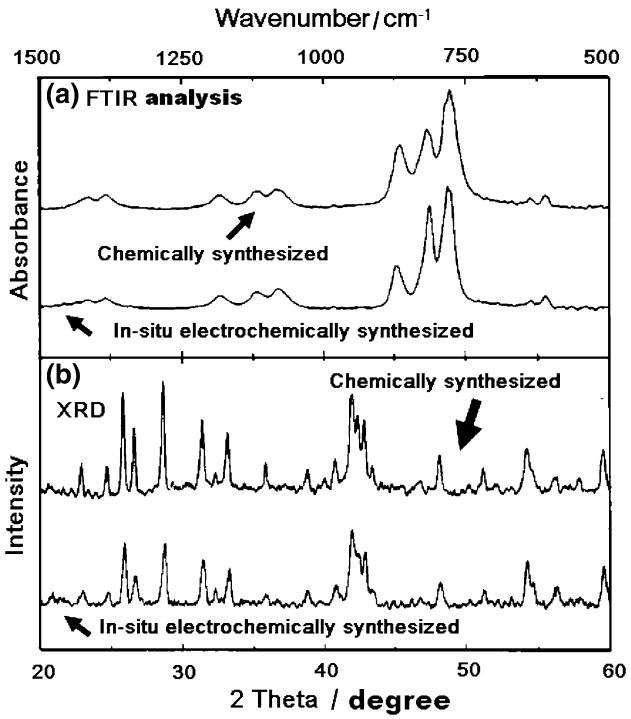

Fig. 5 XRD (bottom) and FTIR (top) spectra of chemically and electrochemically synthesized $BaFeO_4$ [31]

Table 3 In situ electrochemical syntheses of $BaFeO_4$ under a variety of physical and chemical conditions [31]

[NaOH] (M)	[$Ba(OH)_2$] (M)	Electrolysis time (min)	Internal temperature (°C)	n_{Ba}/n_{Fe} in reactants	Theoretical $BaFeO_4$ produced (mmol)	$BaFeO_4$ purity (%)	Yield (%)	Synthesis efficiency (%)
10	50	80	25	1.0:1.0	4.00	74.6	22.6	16.9
14	45	50	25	1.0:1.0	3.60	85.7	25.2	21.6
14	45	45	35	1.0:1.0	3.60	91.6	75.5	69.2
14	45	250	35	1.0:5.5	3.60	74.5	87.6	65.3
14	45	30	45	1.5:1.0	2.40	92.8	60.5	56.1
14	45	45	45	1.0:1.0	3.60	93.8	61.7	57.9
14	45	70	45	1.0:1.5	3.60	94.5	61.9	58.5
14	45	135	45	1.0:3.0	3.60	85.8	74.9	64.3
14	45	45	55	1.0:1.0	3.60	93.4	42.2	39.4

Table 4 Properties of electrochemical in situ, ex situ, and the chemical synthesized $BaFeO_4$ [31]

	Ex situ electrochemically synthesized $BaFeO_4$	In situ electrochemically synthesized $BaFeO_4$	Chemically synthesized $BaFeO_4$
Optimal synthesis conditions	[NaOH] = 10 M, T = 25 °C $0.67 < n_{Ba}/n_{Fe} < 0.33$ $J = 2$ mA cm^{-2}	[NaOH] = 14 M, T = 45 °C $0.67 < n_{Ba}/n_{Fe} < 1.00$ $J = 2$ mA cm^{-2}	3 °C < T < 5 °C $n_{Ba}/n_{Fe} = 1.5$
Synthesis time	90–100 min	45–75 min	17 h (1,000 min)
Purity (%)	90	93–95	95–98
Yield (%)	93–98	61–62	90–97

An interesting aspect of the in situ electrochemically synthesized $BaFeO_4$ is a substantially enhanced stability of the salt as summarized in Fig. 6. Comparing the time-dependent purity of a similar initial purity chemically and electrochemically synthesized $BaFeO_4$, stored under air at 45 °C, reveals a substantially higher stability for the in situ electrochemically synthesized $BaFeO_4$.

The improved stability characteristic of the electrochemically synthesized material may be beneficial towards its utilization in electrochemical storage applications. SEM results indicate that the grain size of the electrochemical synthesized $BaFeO_4$ is substantially smaller, as shown in Fig. 7 [32]. The result is partially explained by the rapid rate of the electrochemical, compared to chemical, synthesis. The rapid synthesis decreases the time in which the salt is exposed to the aqueous synthesis media, decreasing parasitic decomposition reactions. Nevertheless, the synthesis is performed in an aqueous electrolyte which sustains high oxidation rates and permits dissolution of the Fe(VI) intermediate, but exposes the salt to parasitic decompositions. One interesting observation toward an interpretation of the different stabilities evident is the higher trace Mn concentrations of Mn for the in situ electrochemically compared to chemically synthesized $BaFeO_4$ [31]. Manganese can be concurrently oxidized with the iron to form high valence manganese oxide salts, and can stabilize Fe(VI) salts by the renewal of decomposed Fe(III), according to reactions such as [12, 20]:

$$3MnO_4^{2-} + H_2O + Fe_2O_3 \rightarrow 3MnO_2 + 2OH^- + 2FeO_4^{2-} \quad (13)$$

6 In situ electrochemical synthesis of K_2FeO_4

Solubility of K_2FeO_4 is low in the high-concentration alkaline solution. This provides the possibility of direct electrochemical synthesis of solid K_2FeO_4 in alkaline media. In situ electrochemical synthesis of solid K_2FeO_4 was first studied by Lapicque and Valentin [54]. In their study, Mixed KOH–NaOH solutions were employed for the synthesis of solid potassium ferrate. The yield of potassium ferrate was 12 g L^{-1} with current yields of approximately 20% by dissolution of a cast iron anode in a 400 g L^{-1} KOH, 400 g L^{-1} NaOH solution [54].

He et al. systematically studied the one-step electrochemical synthesis of solid K_2FeO_4 [55]. Generally, NaOH is the leading electrolyte for the electrolytic preparation of Fe(VI). However, at the temperatures higher than 50 °C, KOH is also a good electrolyte for the electrolytic preparation of Fe(VI). The anodic reaction can be generalized as:

$$Fe + 8OH^- + 2K^+ \rightarrow K_2FeO_4(s) + 4H_2O + 6e^- \quad (14)$$

At lower temperatures, little Fe(VI) can be electrochemically generated in KOH solution. However, the synthesis progresses rapidly with increasing temperature due to the anode activation from the higher temperature, and

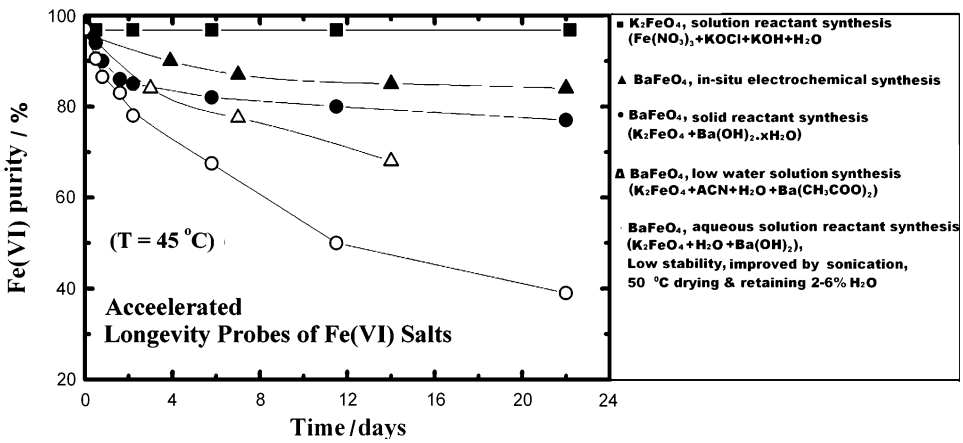

Fig. 6 45 °C stability after storage, of in situ electrochemically synthesized $BaFeO_4$, compared to solid or solution chemically synthesized $BaFeO_4$, and chemically synthesized K_2FeO_4, as determined by chromite analysis [31]

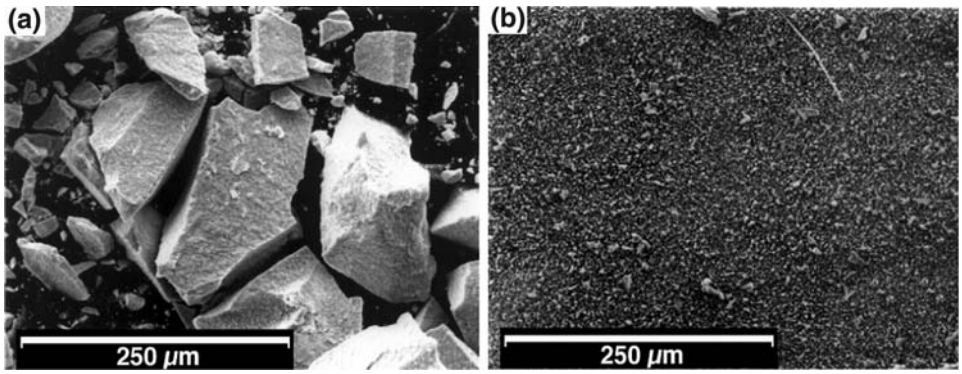

Fig. 7 SEM of chemical (**a**) and electrochemical (**b**) synthesized[7c] $BaFeO_4$. Grain size is stable before and after 45 °C, 30 day storage [32]

mainly forming the solid K_2FeO_4 salt. The comparatively suitable temperature for this synthesis was proved to be 65–75 °C [55]. The effect of KOH concentration and anodic current density, on purity, yield and current efficiency, during the in situ electrochemical synthesis of K_2FeO_4 in KOH solution are summarized in Fig. 8a and b. A significant decrease of the current efficiency can be seen for higher KOH concentrations (Fig. 8a). This is attributed to that the dissolution process of iron anode in more concentrated alkaline solution is slowed down due to the lack of free water in the high-concentration KOH solution [56]. A maximum current efficiency of 73.2% can be obtained at 1.0 mA cm^{-2} current density (Fig. 8b). As shown in Fig. 8b, an obvious decrease of the current efficiency is found with increasing current density, the same but slight decrease trend occurs for both the purity and yield. This is because the electrolysis process of iron anode in higher current density can result in more evolution of oxygen, and more decomposition of Fe(VI) due to the increase in the internal cell temperature with increasing the rate of IR heating [23].

7 Electrochemical synthesis of Fe(III/VI) thin films

Fe(VI) salts, synthesized by solution phase, solid phase and electrochemical method, have been introduced as a novel series of charge storage super-iron salts [10–50]. Whereas primary charge transfer has been extensively demonstrated, reversible charge transfer of super-iron cathodes has been problematic. In principle, a sufficiently thin film Fe(III/VI) cathode should facilitate electronic communication with a conductive substrate to sustain cycled charge storage or reversible deposition. However, a variety of Fe(VI) thin films, formed by pressure and/or mix with a granular conductor such as small grain carbons [29], had passivated upon charge cycling. In 2004, Licht's group first observed that rechargeable Fe(VI/III) films can be generated, by electrodeposition onto conductive substrates from solution phase Fe(VI) electrolytes [32]. A thin film was generated on a smooth Pt foil electrode from micro-pipette controlled, microliter volumes of dissolved Fe(VI) in alkaline solution. It was observed that a nanofilm (for example, a 3 nm thickness Fe(VI) film) formed by electrodeposition was highly reversible [32]. This film was rigorous, and when used as a storage cathode, exhibited charging and discharging potentials characteristic of the Fe(VI) redox couple, and extended, substantial reversibility. Figure 9 is an example of a three Faraday capacity, reversible Fe(VI/III) cathode. A full 80% DOD (depth of discharge) of the 485 mA h g^{-1} capacity Na_2FeO_4 film is readily evident after 100 galvanostatic cycles [32].

Whereas ultra-thin super-iron films can sustain an extended reversibility, thicker films were not rechargeable due to the irreversible buildup of passivating (resistive)

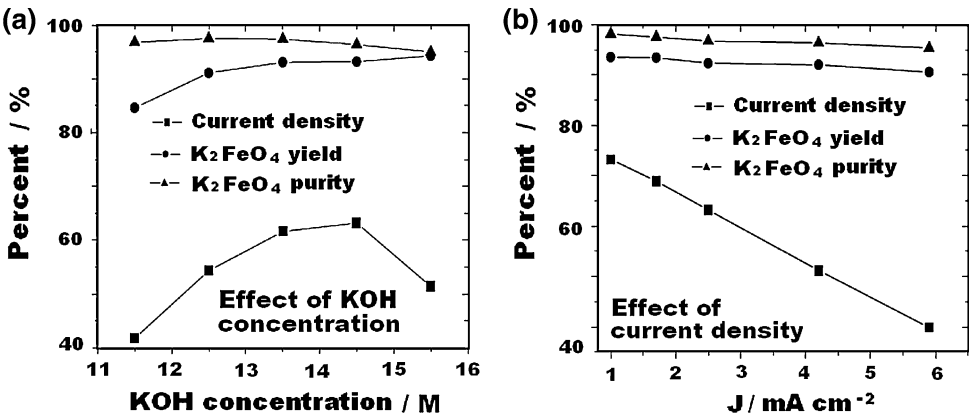

Fig. 8 In situ electrosynthesis of K_2FeO_4 in KOH solution at 65 °C. (**a**) Effect of KOH concentration on purity, yield and current efficiency. (**b**) Effect of apparent current density on purity, yield and current efficiency [55]

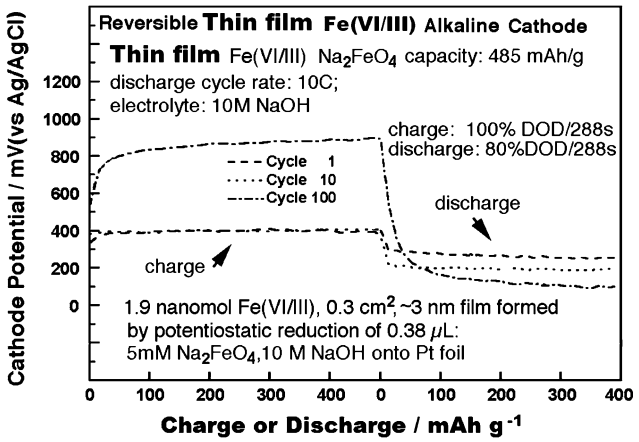

Fig. 9 Reversible charge storage of a Fe(VI) of a 485 mA h g^{-1} capacity Na_2FeO_4 nanofilm [32]

Fe(III) oxide, formed during film reduction. In 2006, Licht's group probed that preparation of Fe(III/VI) films on an extended conductive matrix can facilitate the thick film's reversibility [41]. Substrates for the film preparation are Pt or Ti foil. The extended conductive matrixes are prepared through depositing platinum (or Pt–Au co-deposition) on the substrates. Super-iron films were electrodeposited from 30 mM K_2FeO_4 as dissolved in 10 M NaOH. A substantial improvement to sustain thick film charge transfer was obtained when an extended conductive matrix was utilized as the film substrate. Specially, in a half-cell configuration, a 100 nm Fe(VI) cathode, electrodeposited on the extended conductive matrixes, sustained 100–200 reversible three-electrode galvanostatic charge/discharge cycles, and a 19 nm thin film cathode sustained 500 such cycles. In a full-cell (in conjunction with a metal hydride anode), a 250 nm super-iron film sustained 40 charge/discharge cycles, and a 25 nm film was reversible throughout 300 cycles [41]. Using Ti foil as the substrate, a 50 nm Fe(III) film on 7.5 mg Pt cm^{-2} platinized Ti can sustain over 200 charge/discharge cycles. When Pt–Au codeposited Ti surface was used as the substrate. A 300 nm super-iron film displayed a moderate charge/discharge cycle life of 20 [41].

The facilitated super-iron charge transfer, upon platinization, as a result of the expanded conductive matrix to facilitate charge transfer, is represented in Fig. 10. Without direct contact with the substrate, the shaded Fe(III) centers in Fig. 10a had posed an impediment to charge transfer. This was partially (Fig. 10b) and fully alleviated (Fig. 10c) by intimate contact with the enhanced conductive matrix, which maintains extended direct contact with the substrate [32, 41].

8 Electrochemical methodologies for Fe(VI) analysis

Electroanalytical techniques to probe Fe(VI) compounds can be conveniently categorized as either solution phase

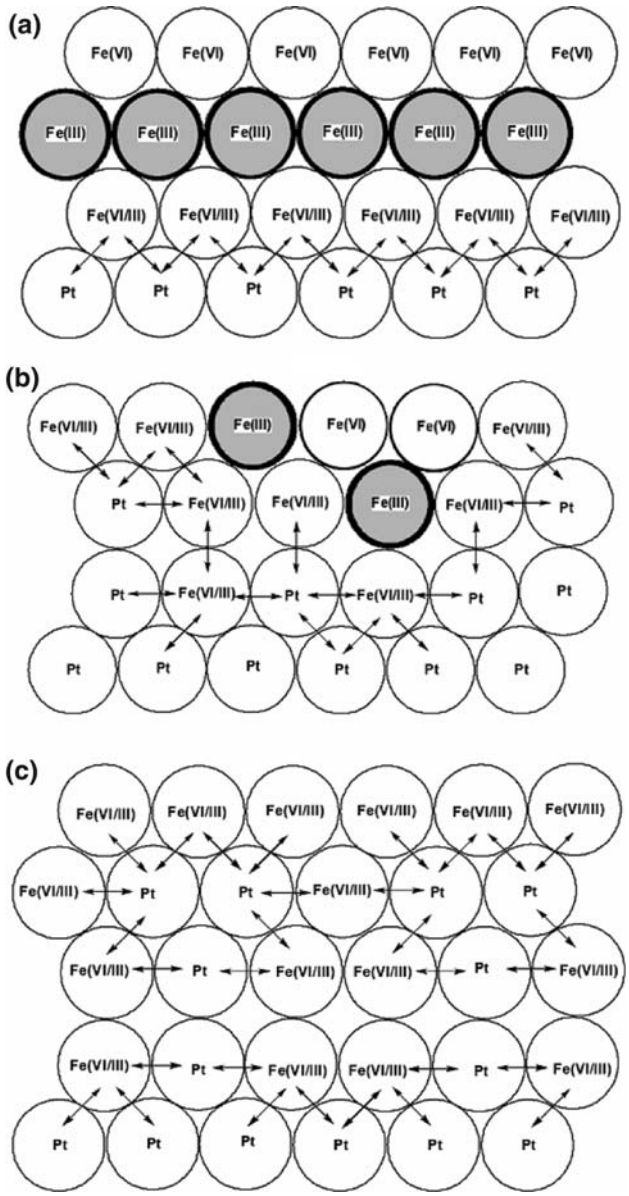

Fig. 10 Representation of Fe(III/VI) passivation (**a**), as well as the partial (**b**) and full (**c**) alleviation through an extended conductive matrix in Fe(III/VI) ferrate films [41]

(dissolved Fe(VI)) or solid cathode techniques. Solution electrochemical techniques such as potentiometric, galvanostatic and cyclic-voltammetry methods are convenient, and can be carried out using a conventional potentiostat in a three-electrode electrochemical cell. Fe(VI) Electrochemical Analyses summarized here include following methodologies.

8.1 Fe(VI) potentiometric analysis

The measured redox potentials, at platinum electrode, of K_2FeO_4 in various NaOH solutions was measured yielding $E°(\text{in NaOH})FeO_4^{2-} = 0.66 \pm 0.01$ V (SHE). As expected,

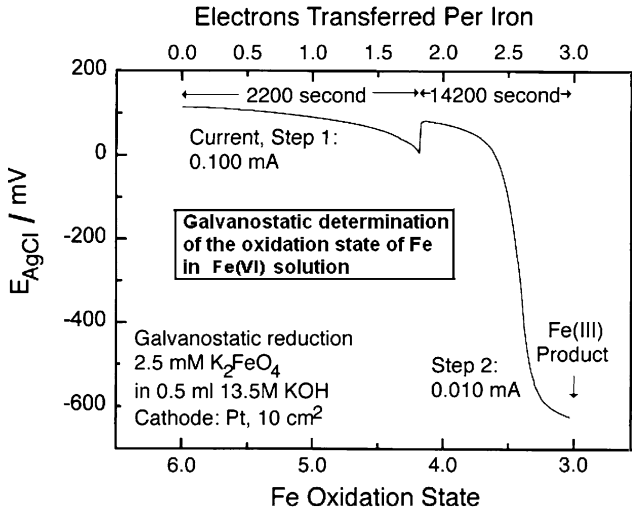

Fig. 11 Galvanostatic determination of the measurement of the oxidation state of iron in ferrate(VI) solutions [17]

redox potential shifts to more positive values with log of the increase in ferrate concentration and was analyzed in detail in reference [17]. In aqueous alkali and alkali earth hydroxide electrolytes, a variety of Fe(VI) compounds, over a wide concentration range, exhibit a potential varying from 0.55 to 0.75 V versus SHE [17].

8.2 Fe(VI) solution phase galvanostatic analysis

Galvanostatic reduction of dissolved ferrate yields a direct electrochemical measurement of the oxidation state of iron in ferrate. Figure 11 presents the time evolution of the potential, during ferrate reduction. A $c_{initial} = 2$ mM potassium ferrate solution in v = 3 mL of 15 M NaOH is reduced at a current density J = 10 μA cm^{-2}. Integration of the charge transferred yields the relative oxidation state, Δq', where F is the Faraday constant and t is time [17]:

$$\Delta q' = t \times J/(c_{initial} \times v \times F) \quad (15)$$

and which may be compared to the intrinsic charge of the insoluble Fe(III) product. A planar platinum electrode does not provide the optimum surface to probe solution phase Fe(VI) reduction. The Pt surface tends to passivate in time as the reduced Fe(III) layer builds on the surface. This passivation is alleviated by (i) minimizing the thickness of the layer, employing low volumes and low concentrations of dissolved Fe(VI) salts, (ii) using low initial current densities, such as 10 μA cm^{-2}, and (iii) further diminishing the current by an order of magnitude as the overpotential increases towards the end of the reduction. Under these conditions, and as seen in the curve in Fig. 11, the oxidation state of the starting material approaches Fe(VI) in accord with Eq. 15.

8.3 Fe(VI) cyclic voltammetry analysis

Representative voltammetric curves for the reduction of K_2FeO_4 dissolved in 15 M NaOH at a Pt electrode are shown in Fig. 12 and are further detailed in reference [17]. The negative potential scan reveals a cathodic current of ferrate(VI) reduction at potentials less positive than 200 mV, and cathodic reduction of ferrate(VI) proceeds with an overvoltage of approximately 150 mV. O_2 evolution in the oxidation sweep interferes with oxidation of ferrate(III). The peak cathodic current density increased linearly with ferrate concentration and was proportional to $(\text{scan rate})^{1/2}$, indicating diffusion limitation of ferrate(VI) reduction.

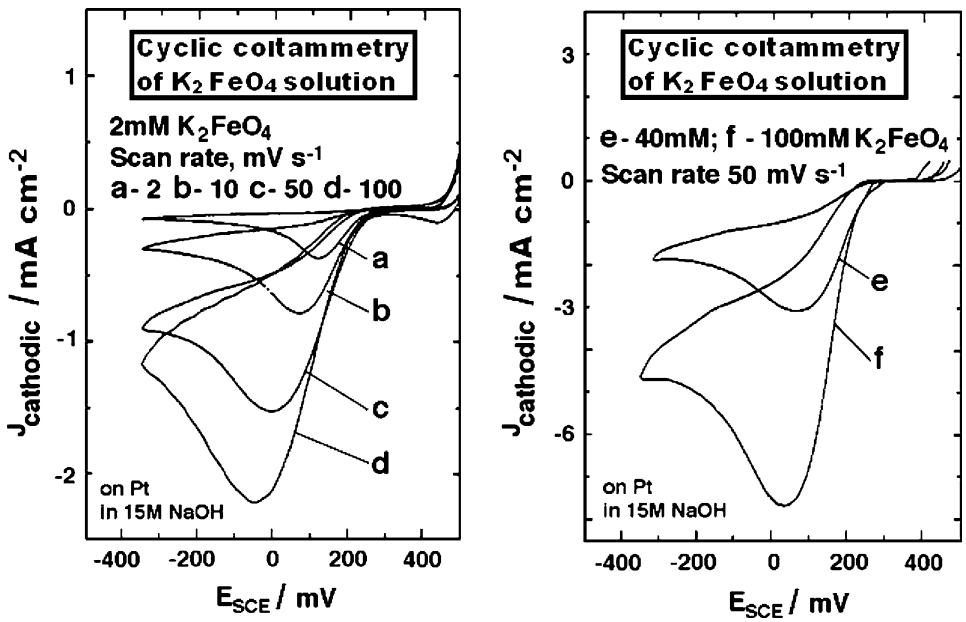

Fig. 12 Cyclic voltammetry of ferrate(VI) solutions. Left: Variation with potential scan rate. Right: Variation with ferrate(VI) concentration [17]

9 Summary

In this review, two electrochemical syntheses (in situ and ex situ) of Fe(VI) salts routs are presented. High purity K_2FeO_4 and $BaFeO_4$ can be efficiently synthesized electrochemically, directly as a solid phase, from concentrated alkaline media. The optimized electrolysis conditions for electrochemical Fe(VI) synthesis are summarized. Direct electrochemical synthesis of Fe(VI) compounds has several advantages of shorter synthesis time, simplicity, reduced costs (no chemical oxidant is required) and providing a possible pathway towards more electroactive and thermal stable Fe(VI) compounds.

Fe(VI) compounds have been explored as energy storage cathode materials in both aqueous and non-aqueous phase in "super-iron" battery configurations. In this paper, electrochemical preparation of reversible Fe(VI/III) thin film towards a rechargeable super-iron cathode is also summarized. Ultra-thin (a few nanometers) Fe(III/VI) films exhibited a high degree of three-electron reversibility (throughout 100–200 charge/discharge cycles), However, thicker films had been increasingly passive toward the Fe(VI) charge transfer. Extended conductive matrix facilitated a two orders of magnitude enhancement in charge storage for reversible Fe(III/VI) thin films.

Electroanalytical techniques to probe Fe(VI) compounds can be conveniently categorized as solution phase. Various electrochemical methodologies for Fe(VI) analysis including potentiometric analysis, galvanostatic analysis and cyclic voltammetry are summarized.

References

1. Carr JD, Kelter PB, Tabatabai A, Splichal D, Erickson J, Mclaughlin CW (1985) In: Jolly RL (ed) Proc. 5th conference of water chlorination. Lewis, Chelsea, p 1285
2. Sharma VK, Smith JO, Millero FJ (1997) Environ Sci Technol 31:2486
3. Licht S, Yu X (2005) Environ Sci Technol 39:8071
4. Jiang JQ (2007) J Hazard Mater 146:617
5. Jiang J, Wang S, Panagoulopoulos A (2007) Desalination 210:266
6. Yngard R, Damrongsiri S, Osathaphan K, Sharma V (2007) Chemosphere 69:729
7. Cho M, Lee Y, Choi W, Chung H, Yoon J (2006) Wat Res 40:3580
8. Jiang J, Wang S, Panagoulopoulos A (2006) Chemosphere 63: 212
9. Delaude L, Laszlo P (1996) J Org Chem 61:6360
10. Licht S, Wang B, Ghosh S (1999) Science 285:1039
11. Licht S, Wang B, Ghosh S, Li J, Naschitz V (1999) Electrochem Comm 1:522
12. Licht S, Wang B, Xu G, Li J, Naschitz V (1999) Electrochem Comm 1:527
13. Licht S, Wang B, Li J, Ghosh S, Tel-Vered R (2000) Electrochem Comm 2:535
14. Licht S, Wang B (2000) Electrochem Solid-State Lett 3:209
15. Licht S, Naschitz V, Ghosh S, Lin L, Liu B (2001) Electrochem Comm 3:340
16. Licht S, Naschitz V, Ghosh S, Liu B, Halperine N, Halperin L, Rozen D (2001) J Power Sources 99:7
17. Licht S, Naschitz V, Lin L, Chen J, Ghosh S, Liu B (2001) J Power Sources 101:167
18. Licht S, Ghosh S, Dong Q (2001) J Electrochem Soc 148:A1072
19. Licht S, Naschitz V, Ghosh S (2001) Electrochem Solid-State Lett 4:A209
20. Licht S, Ghosh S, Naschitz V, Halperin N, Halperin L (2001) J Phys Chem B 105:11933
21. Licht S, Ghosh S (2002) J Power Sources 109:465
22. Licht S, Naschitz V, Ghosh S (2002) J Phys Chem B 106:5947
23. Licht S, Tel-Vered R, Halperin L (2002) Electrochem Comm 4:933
24. Licht S, Naschitz V, Wang B (2002) J Power Sources 109:67
25. Lee J, Tryk D, Fujishima A, Park S (2002) Chem Comm 5:486
26. Yang W, Wang J, Pan T, Xu J, Zhang J, Cao C (2002) Electrochem Comm 4:710
27. Yang W, Wang J, Zhang Z, Zhang J, Cao C (2002) Chin Chem Lett 13:761
28. Tel-Vered R, Rozen D, Licht S (2003) J Electrochem Soc 150:A1671
29. Ghosh S, Wen W, Urian RC, Heath C, Srinivasamurthi V, Reiff W, Mukerjee S, Naschitz V, Licht S (2003) Electrochem Solid-State Lett 6:A260
30. De Koninck M, Brousse T, Belanger D (2003) Electrochim Acta 48:1425
31. Licht S, Tel-Vered R, Halperin L (2004) J Electrochem Soc 151:A31
32. Licht S, Tel-Vered R (2004) Chem Comm 6:628
33. Licht S, Naschitz V, Rozen D, Halperin N (2004) J Electrochem Soc 151:A1147
34. Zhang C, Liu Z, Wu F, Lin L, Qi F (2004) Electrochem Comm 6:1104
35. Walz K, Suyama A, Suyama W, Sene J, Zeltner W, Armacanqui E, Roszkowski A, Anderson M (2004) J Power Sources 134:318
36. Licht S, Yang L, Wang B (2005) Electrochem Comm 7:931
37. Nowik I, Herber RH, Koltypin M, Aurbach D, Licht S (2005) J Phys Chem Solids 66:1307
38. Koltypin M, Licht S, Tel-Vered R, Naschitz V, Aurbach D, (2005) J Power Sources 146:723
39. Ayers K, White N (2005) J Electrochem Soc 152:A467
40. Koltypin M, Licht S, Nowik I, Levi E, Gofer Y, Aurbach D (2006) J Electrochem Soc 153:A32
41. Licht S, DeAlwis C (2006) J Phys Chem B 110:12394
42. Licht S, Yu X, Zheng D (2006) Chem Comm 41:4341
43. Walz K, Szczech J, Suyama A, Suyama W, Stoiber L, Zeltner W, Armacanqui E, Anderson M (2006) J Electrochem Soc 153:A1102
44. Licht S, Yu X, Qu D (2007) Chem Comm 26:2753
45. Yu X, Licht S (2007) J Power Sources 171:966
46. Yu X, Licht S (2007) J Power Sources 171:1010
47. Yu X, Licht S (2007) Electrochim Acta 52:8138
48. Yu X, Licht S (2007) J Power Sources 173:1012
49. Walz K, Handrick A, Szczech J, Stoiber L, Suyama A, Suyama W, Zeltner W, Johnson C, Anderson M (2007) J Power Sources 167:545
50. Xu Z, Wang J, Shao H, Tang Z, Zhang J (2007) Electrochem Comm 9:371
51. Bouzek K, Lipovska M, Schmidt M, Rousar I, Wragg A (1998) Electrochim Acta 44:547
52. De Koninck M, Belanger D (2003) Electrochim Acta 48:1435
53. He W, Wang J, Yang C, Zhang J (2006) Electrochim Acta 51:1967
54. Lapicque F, Valentin G (2002) Electrochem Comm 4:764

55. He W, Wang J, Shao H, Zhang J Cao C (2005) Electrochem Comm 7:607
56. Bouzek K, Rousar I (1997) J Appl Electrochem 27:679
57. Bouzek K, Schmidt M, Wragg A (1999) Electrochem Comm 1:370
58. Licht S, Manassen J (1987) J Electrochem Soc 134:1064
59. Licht S (1985) Anal Chem 57:514
60. Licht S (1998) In: Bard AJ, Rubinstein I (eds) Electroanalytical Chemistry, vol 20. Marcel Dekker, NY, p 87
61. Zou J, Chin D (1988) Electrochim Acta 33:477